The International Journal of Advanced Manufacturing Technology (2018) 96:1377–1392
https://doi.org/10.1007/s00170-018-1682-x

ORIGINAL ARTICLE

Evaluating the effects of as-casted and aged overcasting of Al-Al joints

Muhammad Asad Ali[1] · Mirza Jahanzaib[1] · Ahmad Wasim[1] · Salman Hussain[1] · Nazeer Ahmad Anjum[2]

Received: 11 October 2017 / Accepted: 29 January 2018 / Published online: 12 February 2018

Abstract
This research aims to evaluate Al-Al joints fabricated by overcasting liquid 2024 Al alloy onto Zn-electroplated 2024 Al alloy solid inserts followed by solidification under pressure. The effects of three most influencing process parameters including squeeze pressure, die temperature and melt temperature on the mechanical properties of as-casted and aged overcast joints were investigated. Response surface methodology with central composite design was employed for experimental design and development of empirical models. The observed responses in this research include ultimate tensile strength and hardness. Adequacy and validity of the developed models were verified through ANOVA and confirmation experiments, respectively. For both as-casted and aged overcasting conditions, the results revealed melt temperature as the most significant process parameter affecting ultimate tensile strength and hardness followed by die temperature and squeeze pressure. The comparative analysis of the two conditions suggested aged overcasting as the better alternative which resulted in 5.7~9.8 and 3.6~12.4% improvement in ultimate tensile strength and hardness, respectively.

Keywords Wrought Al alloy · Overcasting · Squeeze casting · Aging · Mechanical properties · Response surface methodology

1 Introduction

Aluminium possesses high strength, formability and permeability characteristics and is therefore considered as ideal candidate for low-weight applications. It is being excessively used in aerospace and automotive industry [1, 2]. With the emergence of innovation and new technologies in industry, aluminium alone cannot fulfill the requirements of industry. Therefore, the demand of metal joining technique is growing rapidly [3]. Currently, both similar and dissimilar metals are being joined through these techniques. These can be classified into three major groups including (1) solid with solid bonding (brazing [4], rolling [5], friction stir welding [6], laser welding [7], explosive welding [8], surface activated bonding [9] and hydrostatic extrusion [10]), (2) solid with liquid bonding (hot dipping [11] and overcasting [12]), and (3) liquid with liquid bonding (continuous casting [13] and direct chill casting [14]). It is worthy to note that solid with solid bonding is a lengthy process and requires high investment for shape and substrate design. Liquid with liquid bonding is also not an economical solution and therefore not commercially suitable for industrial practices [15].

Solid with liquid bonding also termed as overcasting is considered as the best joining technique due to its superior characteristics including high production efficiency, excellent performance, design flexibility, mass saving and low operating cost [16]. Overcasting has emerged as a proven process for joining a variety of dissimilar metals including aluminium (Al) and iron (Fe) alloys [17], semi-solid aluminium (Al) and stainless steel alloys [18], Al and copper (Cu) alloys [12], stainless-steel and structural-alloy-steel [19], magnesium (Mg) and aluminium (Al) bimetallic castings [20], Mg-Al bimetal macro-composite [21], high chromium (Cr)-cast iron and medium carbon (C)-steel bimetal [22, 23], and grey iron and copper (Cu) alloys [24]. The joining of similar metal such as Mg and Mg alloys [25] has also been reported in literature. However, the joining of aluminium-aluminium alloys has not been perfectly achieved due to the presence of aluminium oxide (Al_2O_3) layer on the aluminium alloy surface [16]. This surface layer has much higher melting point (2072 °C) than the molten metal, which limits wettability while pouring

✉ Salman Hussain
salman.hussain@uettaxila.edu.pk

[1] Industrial Engineering Department, University of Engineering and Technology, Taxila, Taxila, Pakistan

[2] Mechanical Engineering Department, University of Engineering and Technology, Taxila, Taxila, Pakistan

of molten material [26]. This problem was addressed by Papsi et al. [16] who replaced high melting point (2072 °C) layer of Al_2O_3 with low melting point (420 °C) zinc coating. When wrought aluminium alloy is used for overcast joint during gravity casting, casting defect including porosity and cracks is formed at interface [27]. Koerner et al. [28] and Rubner et al. [29] successfully addressed these defects in conventional overcasting by applying high pressure during overcasting, also known as squeeze overcasting. This reduction in defects was obtained due to sound metallurgical bonding in the presence of high pressure [3, 30]. A number of researchers have employed squeeze casting to fabricate similar or dissimilar wrought aluminium-alloy overcast joints. Examples include joining of 6101 wrought aluminium with Zn-coated 6101 wrought aluminium [3], and joining of aluminium A356 with zinc-electroplated aluminium 6101 [31]. Heat treatment can also be employed to further enhance the mechanical properties. Wang et al. [14] developed bimetal 8090-3003 joint and reported that hardness of heat-treated joint was more than as-casted joint at the interface. Papsi et al. [16] fabricated the aluminium-aluminium overcasting joint and observed that aging treatment significantly increased the hardness near the interface. Zhang et al. [32] overcasted A356 onto AA6060 extruded plates and revealed that mechanical properties of overcasted joints were increased after aging treatment. The quality of product fabricated through squeeze casting depends upon the mechanical properties which are greatly affected by various process parameters of squeeze casting including squeeze pressure, die temperature, pressure duration, time delay and melt temperature [33–44] as shown in Fig. 1. The figure also represents different approaches employed by previous researches on different materials for both metal joining and squeeze casting. The materials on which these researches have been conducted are shown on lower *x*-axis for metal joining (similar or dissimilar) and upper *x*-axis for single metal manufacturing. *Y*-axis, on the other hand, demonstrates the researches conducted by employing solid-solid bonding, solid-liquid bonding and liquid-liquid bonding. As an example, solid-solid bonding method was used to joint Al 6061 with AlSiCu alloys [4]. The figure also details the process parameters used by researchers. It can be seen from the figure that squeeze pressure, die temperature and melt temperature are important process parameters influencing the mechanical properties of casted aluminium alloys.

It is clearly evident from Fig. 1 that only conventional technique has been employed for overcasted joints. Other widely applied techniques reported in research include factorial design [33], Taguchi method [34–36], Taguchi and genetic algorithm [37, 38], Taguchi and grey rational analysis [39], response surface methodology and genetic algorithm [40], response surface methodology [41, 42], RSM and artificial neural network [43], and fuzzy logic [44]. Out of these techniques, artificial neural network, genetic algorithm and fuzzy logic are soft computing techniques, whereas Taguchi method, factorial design and response surface methodology are statistical techniques. Although soft computing techniques have the capability to effectively predict the responses, however, large amount of data is required. Furthermore, repetitive hit and trials are employed to adjust parameters for obtaining useful responses which is time consuming as evident from the findings of Karnik et al. [45]. Statistical techniques, on the other hand, require less number of experiments to get useful insight. Out of these statistical techniques, Taguchi method and factorial design are employed for screening experiments [46]. Comparatively, response surface methodology is considered as cost-effective technique due to embedded properties of data fitting and estimation using less number of experiments [41, 42, 47].

Aluminium (2000 series) alloys are extensively used in aerospace and heavy transport vehicle structures due to their embedded properties including better damage tolerance and high resistance to fatigue crack growth than other series of aluminium alloys. Wrought aluminium alloy 2024 is being used extensively for many commercial applications including fuselage structures, wing tension members, shear web, ribs and structural parts where fatigue performance, stiffness and excellent strength are required [1, 48]. From the literature review, it has been found that squeeze overcasting to join Al alloys 2024-2024 has not been investigated in greater detail by pervious researchers. It is also evident that aging has the capability to improve certain mechanical properties; however, there exist little or no work-related aging effects on overcast 2024-2024 Al alloy joints. Therefore, the purpose of this work is to evaluate as-casted and aging effects on mechanical properties of overcast aluminium-aluminium alloy joints fabricated through squeeze casting.

2 Experimental details

This section briefly describes material composition, solid inserts preparation and their surface treatment, experimental setup, overcast joints manufacturing and measurements of response variables. The process of overcasting involves pouring of molten metal over solid inserts. In this research, wrought aluminium alloy 2024 has been used for both molten metal and solid inserts due to its commercial significance in automobile and aerospace industry. The chemical composition of wrought aluminium alloy 2024 is provided in Table 1. The same was verified through optical emission spectroscopy.

Wrought aluminium alloy 2024 solid inserts were prepared in the form of rectangular bar having dimensions of 90 mm × 13 mm × 4 mm. After preparation of aluminium solid inserts, their surface was polished with abrasive papers to make the smooth and burs free. Polishing was followed by three steps chemical treatment process (Table 2). The purpose of

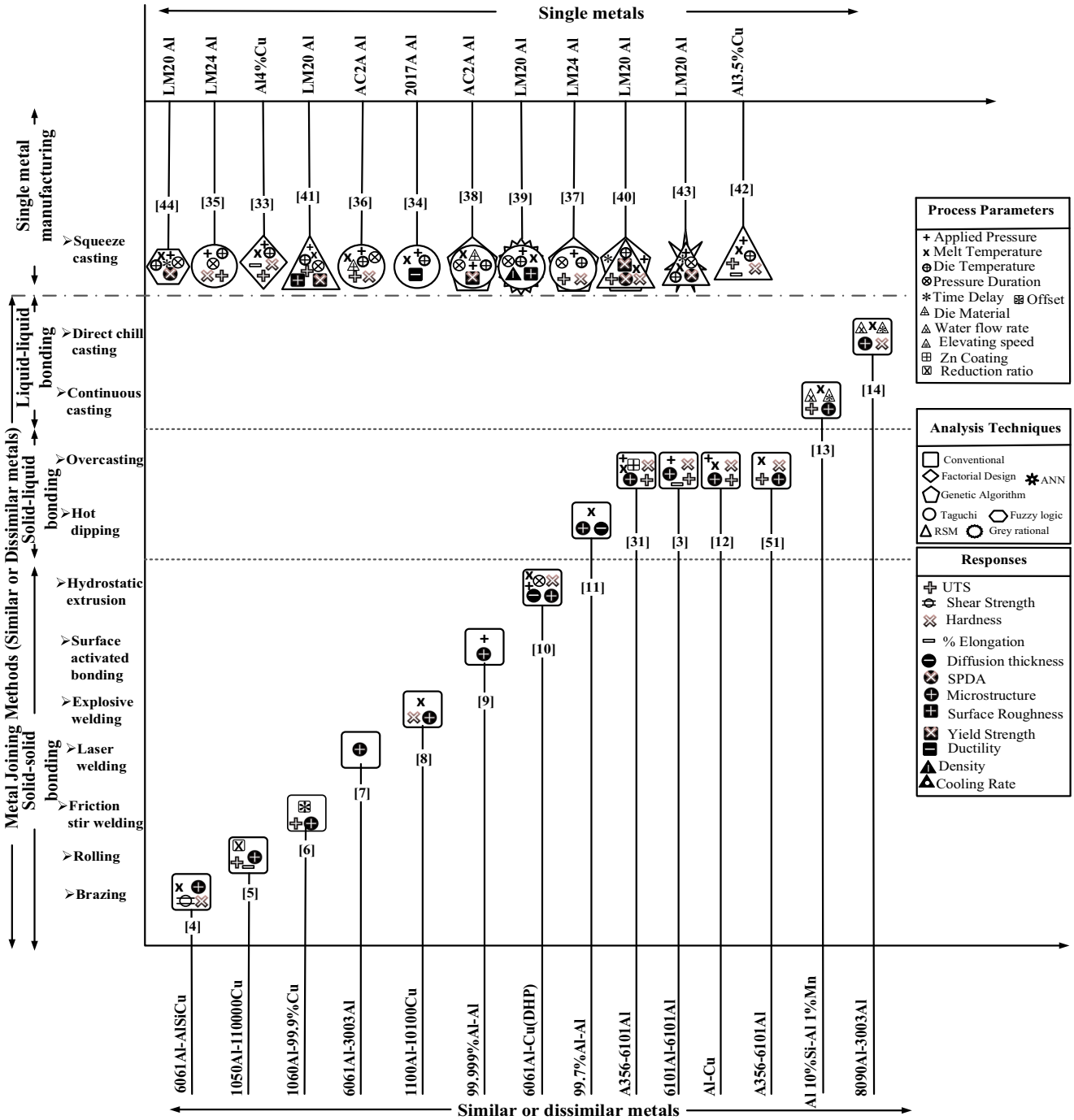

Fig. 1 Overview of previous research on metal joining methods (similar or dissimilar metal), alternative materials and analysis techniques

chemical treatment was to remove the oxides and lubricants from the surface of solid inserts. Since the presence of zinc layer is compulsory for the effective bonding between solid and liquid material in overcasting process, therefore, zincate treatment was performed after the chemical treatment [49, 50]. In zincate treatment process, only 200–300 nm zinc layer was developed on the surface of solid inserts. This minor layer was not enough for effective bonding because of the chances of zinc layer evaporation during the pouring of melt [29]. To overcome this issue, electroplating process was performed on the solid inserts to achieve the zinc layer with 5 μm thickness. It must be noted that 5 μm zinc layer thickness has been

Table 1 Material composition

Elements	Cu	Mg	Mn	Ti	Ni	Si	Al
Weight %	3.85	1.19	0.59	0.02	0.03	0.16	94.16

Table 2 Chemical treatment process

Chemical treatment	Chemical	Operative situation
1. Degreased	C_3H_6O	Ambient temperature, ultrasonic cleaning for 5 min
2. Alkali etching	Strong alkaline solution NaOH (100 g/l, pH > 13)	For 1 min at 55 °C
3. Acid pickling	50% HNO_3	Room temperature for 30 s

reported as the optimum thickness to achieve strong bonding between solid inserts and molten metal [3, 31, 51].

Three squeeze overcasting process parameters including squeeze pressure (SP), die temperature (DT) and melt temperature (MT) were selected in this research. The upper and lower levels of parameters values were selected on the basis of trial runs. Special care was made to ensure defect free bond. The process parameters along with their levels are provided in Table 3.

Experiments were performed based on central composite design (CCD) matrix using response surface methodology (RSM). Overall, 17 experiments were performed with three process parameters each at three levels. Overcasting was performed using vertical hydraulic press having 100 t capacity. H13 forged steel die was used for the squeezing of melt. The following procedure was adopted for overcasting: (i) First of all, the wrought aluminium alloy 2024 was melted in electric resistance furnace having heating capacity of 1200 °C at 5 kW, and (ii) preheating of die was performed prior to the melting process. Zinc-coated solid insert with ejection pin was fitted in the base plate of die before preheating of die. The die was preheated with oxyacetylene torch, whose temperature was measured with infrared thermometer (SMART-SENSOR: AR330). (iii) Once the required temperature of melt and die was achieved, the melt was poured in die followed by application of pressure. (iv) The pressure was maintained until the solidification of melt. After solidification, the pressure was released and billet was removed from the die. Finally, ejection pin was removed from the billet. The schematic illustration of overcasting process along with casted billets (140 mm length × 62 mm diameter) is presented in Fig. 2a, b respectively.

The observed responses for this research include ultimate tensile strength and hardness. Samples for ultimate tensile strength and hardness testing were extracted from the billets by using Milling Machine and EDM Die Sink Machine, according to the ASTM standard: E8/E8M-11 and E384-11, respectively (Fig. 2c–e). It is pertinent to mention that tensile sample of Al 2024-2024 overcast joint material constitutes a sandwich structure (squeeze cast 2024-2024 solid insert-squeeze cast 2024) in the gauge section as presented in Fig. 2d.

Overcasting experiments were performed at (i) as-casted and (ii) aged conditions. In as-casted condition, the samples were extracted from the overcast billets without any additional treatment. In aged treated, on other hand, samples were overcasted followed by heat treatment in the order (a) solution treatment of samples at 500 °C for 2 h, (b) quenching of samples in cold water and (c) artificial aging of samples at 170 °C for 2.5 h.

Ultimate tensile strength was measured using 810-Material Test System (MTS) having capacity of 100 KN at ambient temperature and strain rate of 0.005 mm/s. Three tensile samples were tested for each experimental run, and the average was taken as observed ultimate tensile strength. Stress-strain curve for 2024-2024 overcast joint material under as-casted condition for experimental run (No. 9) is provided in Fig. 3. It is clear from the figure that maximum strength was achieved at 202 MPa, which is termed as ultimate tensile strength. The hardness was measured using Micro Vickers hardness test machine (HV-1000). For measurement, a load of 0.2 KN was applied for 10 s and the hardness was measured on HV scale. For each experimental run, the hardness was measured at three randomly chosen points along the joint. The average was used as final hardness value. The designed experiments along with observed responses and their standard deviation have been provided in Table 4.

Table 3 Process parameters with their levels

Process parameters	Levels			
	Units	Low	Medium	High
Squeeze pressure (SP)	MPa	50	90	130
Die temperature (DT)	°C	150	200	250
Melt temperature (MT)	°C	750	800	850

3 Results and discussions

The present section provides detail regarding development of empirical models, validation of developed models, their analysis using response surface plots and comparison of as-casted with aged 2024-2024 overcast joints.

3.1 Development of empirical models

Empirical models for observed responses (ultimate tensile strength and hardness) have been developed through

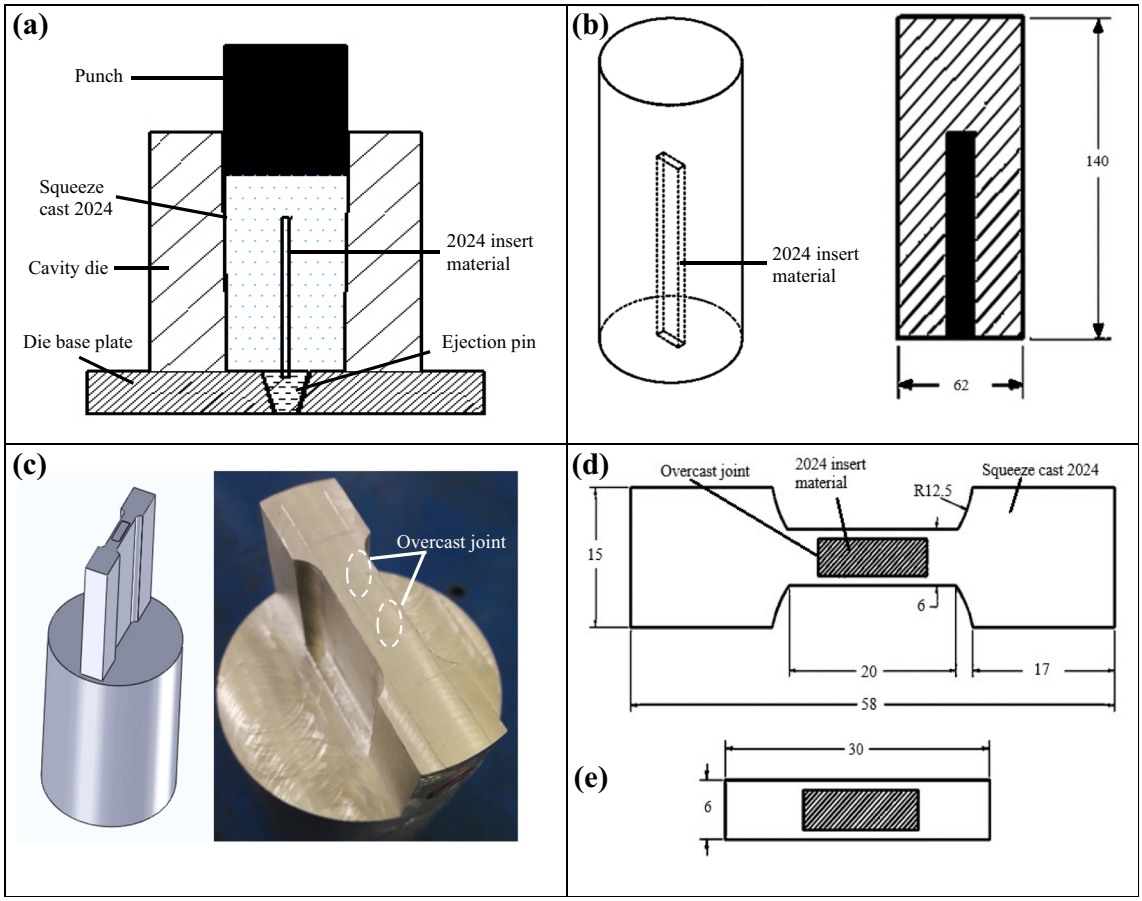

Fig. 2 Schematic illustration of **a** overcast joint process, **b** casted billet, **c** machined billet, **d** dimension of tensile sample in mm and **e** dimension of hardness sample in mm

regression analysis for both as-casted and aged overcast conditions. The adequacy of developed models was verified using analysis of variance (ANOVA) technique. ANOVA has been carried out to determine the impact of process parameters and their interactions on the individual response and to identify the statistical significance [52, 53]. ANOVA can be applied for both continuous (numeric) and categorical input variables [46, 54]. Important terms involved for conducting analysis of variance include degree of freedom (*df*), sum of squares (S.S), means squares (M.S) and *p* value. The *p* value is measured through degree of freedom, sum of squares and means squares. The comparison of observed value with desired significance level indicates the significance of investigated parameter. In response surface methodology, the model is first developed and checked for its significance by using ANOVA. Related information including the significant process parameters are then identified (if model is found significant) using analysis of variance method described earlier [54–57]. Statistical adequacy of developed models is tested with the help of ANOVA, if adequacy measures R^2 (correlation coefficient), adjusted R^2 and predicted R^2 are used. The adequacy is the measure of prediction capability of the developed models [40, 42, 58, 59].

3.1.1 Ultimate tensile strength (UTS)

For both as-casted and aged overcast conditions, the fit summary suggests quadratic relationship as the best fit model. For as-casted 2024-2024 overcast joints, ANOVA results revealed that main and quadratic effects including squeeze pressure, die temperature, melt temperature, (squeeze pressure)^2 and (melt temperature)^2 were significant model terms. For aged

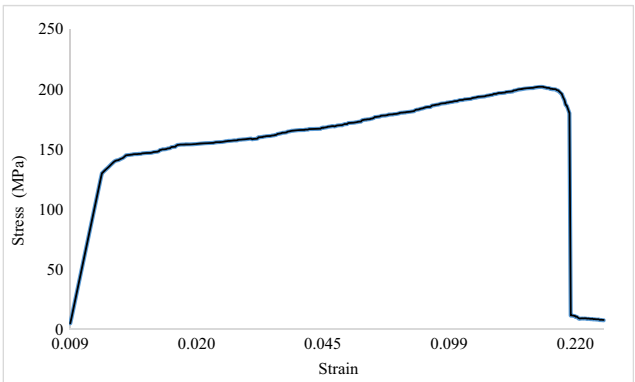

Fig. 3 Stress-strain curve for Al 2024-2024 overcast joint (as-casted experiment run no. 9)

Table 4 Design of experiments (DOE) with observed responses

Run no.	Process parameters			Observed responses							
	Squeeze pressure (MPa)	Die temperature (°C)	Melt temperature (°C)	Ultimate tensile strength (MPa)				Hardness (HV)			
				As-casted Avg.	S.D	Aged Avg.	S.D	As-casted Avg.	S.D	Aged Avg.	S.D
1	50	250	750	214	1.09	235	0.89	90	0.38	98	2.31
2	130	200	800	253	2.18	272	2.07	115	2.81	120	4.02
3	90	150	800	247	1.38	267	4.01	109	3.81	116	3.19
4	130	250	750	237	0.67	257	2.36	93	2.91	103	2.04
5	50	150	850	218	3.01	238	0.39	92	0.96	100	2.18
6	50	150	750	185	2.49	205	1.89	90	0.91	97	1.81
7	130	150	850	245	2.97	265	1.35	104	1.29	111	1.09
8	90	200	800	263	1.06	281	1.93	111	3.07	118	4.01
9	130	150	750	202	0.98	222	0.95	92	4.21	98	3.91
10	50	250	850	247	1.04	267	4.03	99	3.48	113	0.98
11	130	250	850	258	4.05	279	3.59	118	2.49	125	1.39
12	50	200	800	236	3.89	256	1.39	105	1.02	112	4.89
13	90	200	850	255	2.89	275	1.93	106	1.92	110	2.74
14	90	200	800	265	3.62	283	2.94	114	2.47	121	2.95
15	90	200	750	225	1.03	245	3.01	91	3.91	98	3.05
16	90	250	800	280	0.92	297	2.49	121	2.81	128	2.07
17	90	200	800	262	3.8	282	4.06	113	1.91	118	4.25

Standard deviation = Average value − observed value /no. observed values

Avg. average, *SD* standard deviation

overcast condition, an additional interaction effect of (die temperature × melt temperature) has been found significant. Other model terms were insignificant for both conditions and therefore eliminated to improve model adequacy. ANOVA for ultimate tensile strength has been provided in Table 5. The results show that UTS models for both conditions are significant (p values are less than 0.05). The value of adequacy measure R^2, adjusted R^2 and predicted R^2 are close to 1, which indicate the adequacy of the developed models. The developed empirical models for the prediction of ultimate tensile strength under as-casted and aged 2024-2024 overcast joints are presented in Eqs. (1) and (2).

$$\begin{aligned}\mathrm{UTS(As{-}casted)} = {} & -5850.31435 + (2.38530 \times \text{Squeeze Pressure}) + (0.90890 \times \text{Die Temperature}) + \\ & (14.36984 \times \text{Melt Temperature}) - (0.0000625 \times \text{Squeeze Pressure} \times \text{Die Temperature}) - \\ & (0.000125 \times \text{Squeeze Pressure} \times \text{Melt Temperature}) - (0.0011 \times \text{Die Temperature} \times \text{Melt Temperature}) - \\ & (0.010682 \times \text{Squeeze Pressure}^2) + (0.00076338 \times \text{Die Temperature}^2) - (0.00863662 \times \text{Melt Temperature}^2)\end{aligned} \tag{1}$$

$$\begin{aligned}\mathrm{UTS(Aged)} = {} & -5524.57007 + (2.20754 \times \text{Squeeze Pressure}) + (0.95986 \times \text{Die Temperature}) + \\ & (13.61042 \times \text{Melt Temperature}) - (0.0000625 \times \text{Squeeze Pressure} \times \text{Die Temperature}) + \\ & (0.00 \times \text{Squeeze Pressure} \times \text{Melt Temperature}) - (0.0011 \times \text{Die Temperature} \times \text{Melt Temperature}) - \\ & (0.010264 \times \text{Squeeze Pressure}^2) + (0.000630986 \times \text{Die Temperature}^2) - (0.00816901 \times \text{Melt Temperature}^2)\end{aligned} \tag{2}$$

3.1.2 Hardness

The fit summary for hardness suggested quadratic relationship as the best fit model for both the overcasting conditions. ANOVA results highlight that main effects of squeeze pressure, die temperature, melt temperature, interaction effects of (squeeze pressure × melt temperature), (die temperature × melt temperature), and quadratic effects of (squeeze pressure)^2 and (melt temperature)^2 are the significant model terms associated with the hardness while considering as-casted

Table 5 ANOVA for ultimate tensile strength (UTS) under as-casted and aged overcast conditions for 2024-2024 aluminium joints

Source	Ultimate tensile strength (as-casted)						Source	Ultimate tensile strength (aged)					
	df	S.S	M.S	*F*-value	*p* value			*df*	S.S	M.S	*F*-value	*p* value	
Model	9	9855.87	1095.1	81.85	< 0.0001	Significant	Model	9	9433.5	1048.2	107.25	< 0.0001	Significant
A-Squeeze pressure	1	902.50	902.5	67.45	< 0.0001		A-Squeeze pressure	1	883.6	883.60	90.42	< 0.0001	
B-Die temperature	1	1932.1	1932.1	144.4	< 0.0001		B-Die temperature	1	1904.4	1904.4	194.87	< 0.0001	
C-Melt temperature	1	2560	2560	191.3	< 0.0001		C-Melt temperature	1	2560	2560	261.96	< 0.0001	
							BC	1	60.5	60.50	6.19	0.0417	
A^2	1	782.66	782.66	58.49	0.0001		A^2	1	722.59	722.59	73.94	< 0.0001	
C^2	1	1249.1	1249.1	93.35	< 0.0001		C^2	1	1117.5	1117.5	114.35	< 0.0001	
Residual	7	93.66	13.38				Residual	7	68.41	9.77			
Lack of fit	5	88.99	17.8	7.63	0.1199	Not significant	Lack of fit	5	66.41	13.28	13.28	0.0715	Not significant
Pure error	2	4.67	2.33				Pure error	2	2	1			
Cor total	16	9949.53					Cor total	16	9501.9				
Std. dev.	3.6579		R-squared		0.9906		Std. dev.	3.1261		R-squared		0.9928	
Mean	240.7059		Adj R-squared		0.9785		Mean	260.3529		Adj R-squared		0.9835	
C.V. %	1.5196		Pred R-squared		0.8345		C.V. %	1.2007		Pred R-squared		0.8632	
PRESS	1646.5430		Adeq precision		34.3020		PRESS	1299.9531		Adeq precision		39.1408	

Table 6 ANOVA for hardness under as-casted and aged overcast conditions for 2024-2024 aluminium joints

Source	Hardness (as-casted)						Source	Hardness (aged)					
	df	S.S	M.S	*F*-value	*p* value			*df*	S.S	M.S	*F*-value	*p* value	
Model	9	1829.18	203.24	46.88	< 0.0001	Significant	Model	9	1668.4	185.38	89.54	< 0.0001	Significant
A-Squeeze pressure	1	211.60	211.60	48.80	0.0002		A-Squeeze pressure	1	136.90	136.90	66.12	< 0.0001	
B-Die temperature	1	115.60	115.60	26.66	0.0013		B-Die temperature	1	202.50	202.50	97.81	< 0.0001	
C-Melt temperature	1	396.90	396.90	91.54	< 0.0001		C-Melt temperature	1	422.50	422.50	204.07	< 0.0001	
AC	1	84.50	84.50	19.49	0.0031		AC	1	36.13	36.13	17.45	0.0042	
BC	1	50.00	50.00	11.53	0.0115		BC	1	55.13	55.13	26.63	0.0013	
A^2	1	24.57	24.57	5.67	0.0489		A^2	1	14.91	14.91	7.20	0.0314	
							B^2	1	35.52	35.52	17.15	0.0043	
C^2	1	565.50	565.50	130.4	< 0.0001		C^2	1	552.42	552.42	266.82	< 0.0001	
Residual	7	30.35	4.34				Residual	7	14.49	2.07			
Lack of fit	5	25.68	5.14	2.20	0.3412	Not significant	Lack of fit	5	8.49	1.70	0.57	0.7371	Not significant
Pure error	2	4.67	2.33				Pure error	2	6	3			
Cor total	16	1859.53					Cor total	16	1682.9				
Std. dev.	2.0823		R-squared		0.9837		Std. dev.	1.4389		R-squared		0.9914	
Mean	103.7059		Adj R-squared		0.9627		Mean	110.9412		Adj R-squared		0.9803	
C.V. %	2.0079		Pred R-squared		0.8466		C.V. %	1.2970		Pred R-squared		0.9454	
PRESS	285.2861		Adeq precision		18.0336		PRESS	91.9101		Adeq precision		27.6768	

df degree of freedom, *S.S* sum of squares, *M.S* mean square

Table 7 Comparison between actual and predicted values of ultimate tensile strength and hardness for as-cast and aged overcast 2024-2024 joints

SR no.	Process parameters				Response results			
	Squeeze pressure (MPa)	Die temperature (°C)	Melt temperature (°C)		UTS (MPa)		Hardness (HV)	
					As-casted	Aged	As-casted	Aged
1	70	170	780	Actual	236.58	248.92	103.12	115.90
				Predicted	234.72	253.88	105.19	111.15
				% Error	0.79	1.95	1.97	4.27
2	110	220	830	Actual	270.90	282.90	113.90	119.60
				Predicted	269.52	288.80	116.42	122.39
				% Error	0.51	2.04	2.16	2.28
3	70	170	830	Actual	245.90	261.30	102.89	110.60
				Predicted	248.18	267.44	105.46	112.14
				% Error	0.92	2.30	2.44	1.37
4	110	220	780	Actual	265.48	272.70	109.37	118.60
				Predicted	259.07	277.98	110.39	116.66
				% Error	2.47	1.90	0.92	1.65
5	110	170	830	Actual	255.90	269.70	113.04	119.7
				Predicted	258.28	277.59	111.41	116.74
				% Error	0.92	2.84	1.46	2.55
6	70	220	780	Actual	248.90	266.10	108.93	112
				Predicted	249.97	269.08	106.69	113.56
				% Error	0.43	1.11	2.10	1.42
7	110	170	780	Actual	247.8	268.90	105.21	108.7
				Predicted	245.07	264.03	107.89	113.62
				% Error	1.11	1.84	2.48	4.36
8	70	220	830	Actual	254.10	280.30	107.99	120.7
				Predicted	260.67	279.90	109.47	117.17
				% Error	2.52	0.14	1.35	3.01

aluminium alloy 2024-2024 joints. For aged overcast joints, main, interaction and quadratic effects include squeeze pressure, die temperature, melt temperature, (squeeze pressure and melt temperature), (die temperature and melt temperature), (squeeze pressure)^2, (die temperature)^2 and (melt temperature)^2. The ANOVA results of hardness after elimination of insignificant model terms are presented in Table 6. The adequacy measures R^2, adjusted R^2 and predicted R^2 are closer to one which indicates the adequacy of the developed models. The empirical models for the prediction of hardness under as-casted and aged overcasting conditions are provided in Eqs. (3) and (4), respectively.

$$\begin{aligned}\text{Hardness(As-casted)} = &-3428.86884-(0.94433 \times \text{Squeeze Pressure})-(1.09249 \times \text{Die Temperature})+\\ &(9.07778 \times \text{Melt Temperature}) + (0.0005 \times \text{Squeeze Pressure} \times \text{Die Temperature})+\\ &(0.001625 \times \text{Squeeze Pressure} \times \text{Melt Temperature}) + (0.001 \times \text{Die Temperature} \times \text{Melt Temperature})\\ &-(0.00189261 \times \text{Squeeze Pressure}^2) + (0.000788732 \times \text{Die Temperature}^2)-\\ &(0.00581127 \times \text{Melt Temperature}^2)\end{aligned} \tag{3}$$

$$\begin{aligned}\text{Hardness(Aged)} = &-3391.19956-(0.55460 \times \text{Squeeze Pressure})-(1.36066 \times \text{Die Temperature})+\\ &(9.01423 \times \text{Melt Temperature}) + (0.0003125 \times \text{Squeeze Pressure} \times \text{Die Temperature})+\\ &(0.0010625 \times \text{Squeeze Pressure} \times \text{Melt Temperature}) + (0.00105 \times \text{Die Temperature} \times \text{Melt Temperature})-\\ &(0.00147447 \times \text{Squeeze Pressure}^2) + (0.00145634 \times \text{Die Temperature}^2)-(0.00574366 \times \text{Melt Temperature}^2)\end{aligned} \tag{4}$$

3.2 Validation of the developed empirical models

To validate the empirical models developed for both the overcast conditions, eight confirmation experiments were conducted. The values of process parameters for the experiments were chosen from the design space, which were different from those used for model development. To clearly visualize the difference between actual and predicted values, the percentage error was calculated using Eq. 5 [60]. The validation results of empirical models developed for ultimate tensile strength and hardness under as-casted and aged conditions are provided in Table 7.

$$\text{Percentage error} = \left|\frac{\text{actual value}-\text{predicted value}}{\text{predicted value}}\right| \times 100 \tag{5}$$

It is evident from Table 7 that percentage error is less than 5%, which indicates the validity of the developed empirical models. It can be established from the validation results that developed models have the capability to predict the responses accurately with minor deviation.

3.3 Response surface plots

The variations in effects of process parameters (squeeze pressure, die temperature and melt temperature) on the response variables (ultimate tensile strength and hardness) for both the as-casted and aged overcast joints have been analysed using 3D response surface plots. It must be noted that these surface plots elaborates the effect of two process parameters at the central levels of third process parameter.

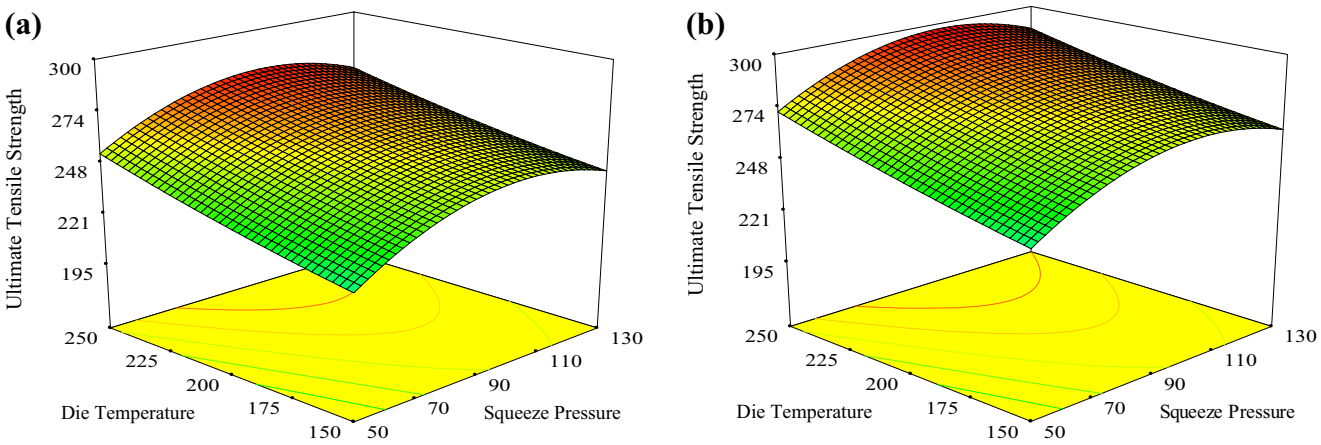

Fig. 4 Response surface plots showing the effects of squeeze pressure and die temperature on ultimate tensile strength for **a** as-casted overcast joints and **b** aged overcast joints

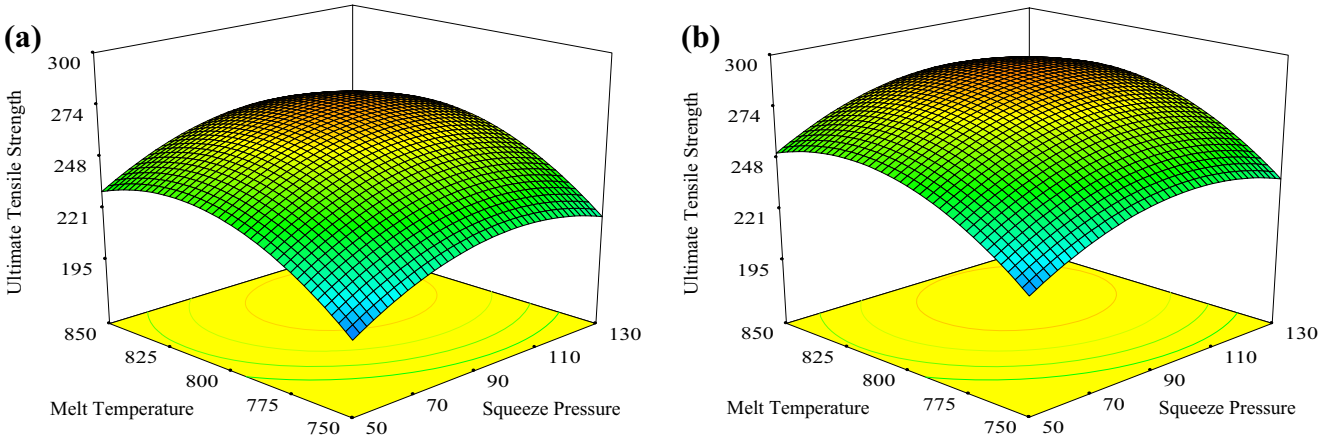

Fig. 5 Response surface plots showing the effects of squeeze pressure and melt temperature on ultimate tensile strength for **a** as-casted overcast joints and **b** Aged overcast joints

3.3.1 Response surface plots for ultimate tensile strength (UTS)

Figure 4a, b represents the effects of squeeze pressure and die temperature on the ultimate tensile strength for as-casted and aged overcast 2024-2024 joints, respectively. While comparing these responses, it can be observed that the varying effects of squeeze pressure and die temperature on the ultimate tensile strength are similar. Ultimate tensile strength is more sensitive to variation in die temperature as compared to squeeze pressure. Furthermore, ultimate tensile strength has non-linear relation with squeeze pressure, while linear relation with die temperature. Ultimate tensile strength increases with increase in die temperature. Furthermore, ultimate tensile strength increases with increase in squeeze pressure up to a certain level and then decreases with further increase in squeeze pressure. It is pertinent to mention that highest ultimate tensile strength of 297.48 MPa has been achieved for aged overcast joints as compared to ultimate tensile strength of 279.14 MPa achieved in as-casted overcast joints.

The effects of squeeze pressure and melt temperature on ultimate tensile strength for as-casted and aged overcast joints are presented in Fig. 5a, b, respectively. It is evident from the figures that the ultimate tensile strength is non-linearly related with squeeze pressure and melt temperature. Ultimate tensile strength increases with increase in squeeze pressure to a certain level and then decreases; similar behaviour can be observed by increasing melt temperature. Furthermore, the effects of melt temperature and squeeze pressure on aged overcast joints are 6.65% higher than as-casted overcast joints.

Figure 6a, b demonstrates the effects of die temperature and melt temperature for both overcast joints conditions. It is clearly evident that ultimate tensile strength relates non-linear with melt temperature and linear with die temperature. Ultimate tensile strength is maximum at middle levels of melt temperature; contemporarily, it increases with increase in die temperature. Similar trend is observed for aged overcast joints. It is observed that melt temperature significantly affects the ultimate tensile strength as compared to the die temperature.

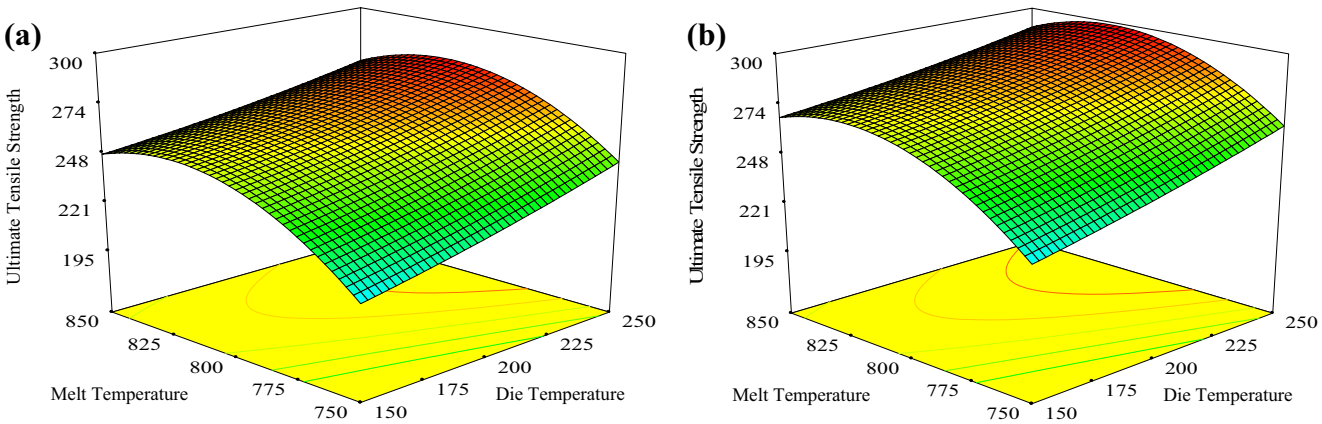

Fig. 6 Response surface plots showing the effects of die temperature and melt temperature on ultimate tensile strength for **a** as-casted overcast joints and **b** aged overcast joints

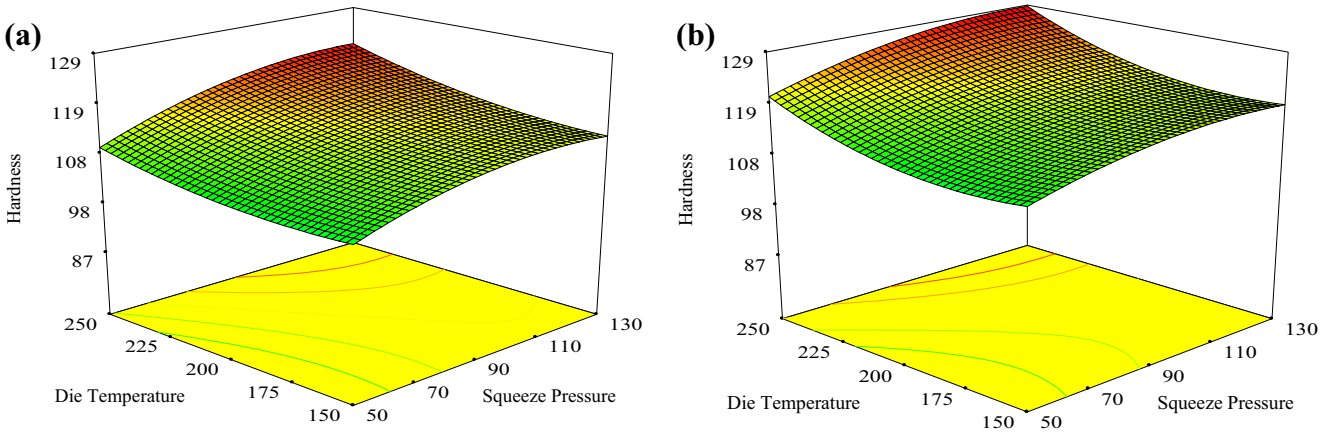

Fig. 7 Response surface plots showing the effects of squeeze pressure and die temperature on hardness for **a** as-casted overcast joints and **b** aged overcast joints

3.3.2 Response surface plots for hardness

The 3D response surface plot demonstrating the effects of squeeze pressure and die temperature on the hardness for as-casted joints (Fig. 7a) is similar to aged overcast joints (Fig. 7b). The response surface plots depict the direct influence of squeeze pressure and die temperature on hardness. It can be observed that hardness for as-casted overcasted is affected more by squeeze pressure than die temperature. While for aged condition, influence of die temperature is more than the squeeze pressure on hardness. For both conditions, hardness increases with increase in die temperature. While with increase in squeeze pressure, hardness increases up to a certain value and then decreases.

Figure 8a, b demonstrates the effects of melt temperature and squeeze pressure on hardness. By comparing these plots, it is clearly evident that similar behaviour of hardness can be observed by varying squeeze pressure and melt temperature. It is clear from the plots that melt temperature significantly affects hardness as compared to squeeze pressure. Hardness increases with the increase in both squeeze pressure and melt temperature up to a certain level, and further increase in these process parameters results in decrease.

The effects of die temperature and melt temperature on hardness are presented in Fig. 9a, b. The figures indicate that hardness is minimum at low levels of die temperature and melt temperature and vice versa. Furthermore, the effect of melt temperature is very large as compared to die temperature.

From the 3D response surface plots, it can be observed that at low levels of squeeze pressure, die temperature and melt temperature, low values of ultimate tensile strength and hardness can only be achieved. This is due to premature solidification at low squeeze pressure and die temperature [40] and incomplete diffusion of two metals because of improper melting of zinc coating at low melt temperature [51]. Similarly, at highest levels of melt temperature and squeeze pressure, low values of ultimate tensile strength and hardness are attained due to the fact that melting of Zn at excessive high temperature occurs which ultimately results in poor metallurgical bonding [31, 51]. Furthermore, higher pressure levels yield the propagation of micro crakes and reduced mechanical properties [61], because at higher levels of pressure and

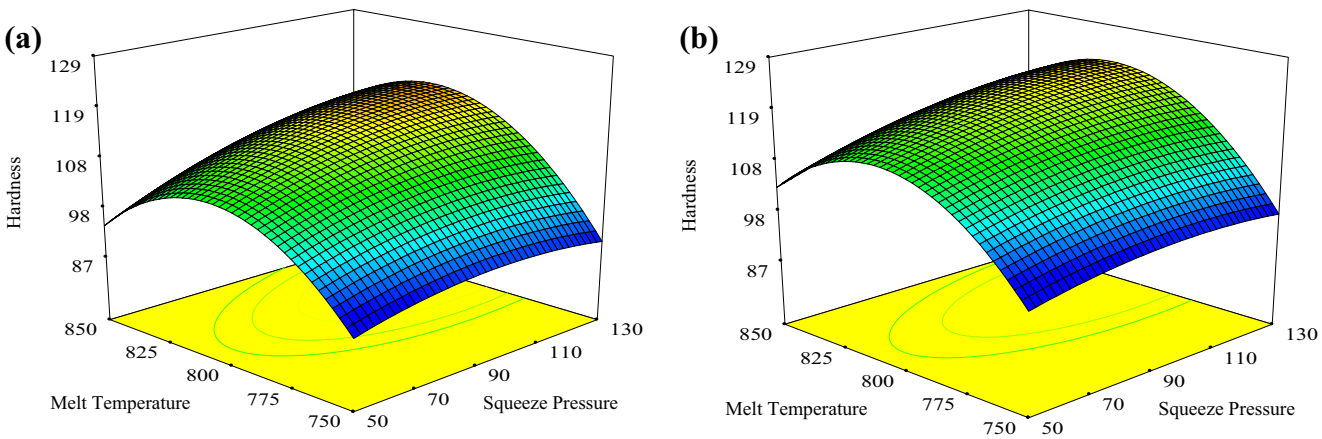

Fig. 8 Response surface plots showing the effects of squeeze pressure and melt temperature on hardness for **a** as-casted overcast joints and **b** aged overcast joints

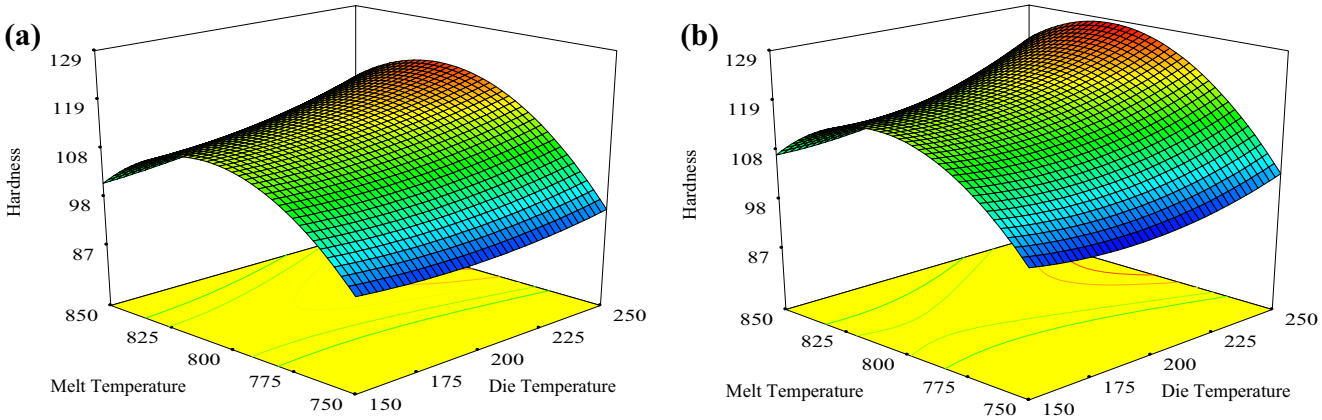

Fig. 9 Response surface plots showing the effects of squeeze pressure and melt temperature on hardness for **a** as-casted overcast joints and **b** aged overcast joints

temperature, diffusion of one metal to other was disturbed due to micro crakes [10].

The above discussion represents the main, interaction and quadratic effects of process parameters (squeeze pressure, die temperature and melt temperature) on the response variables (ultimate tensile strength and hardness). There is always a need to control these process parameters in such a manner that optimum results could be attained. Table 8 represents the summary of main, interaction and quadratic factors affecting the response variables for both overcast joint conditions.

It is clear from Table 8 that main factors (squeeze pressure, die temperature and melt temperature) significantly affect the response variables. The interaction factor (squeeze pressure × melt temperature) influences hardness for both as-casted and aged overcast conditions, whereas (die temperature × melt temperature) affects all response variables except ultimate tensile strength for as-casted overcast joints. The quadratic factors (squeeze pressure)^2 and (melt temperature)^2 influence all response variables, whereas hardness under aged overcast joints condition is influenced by (die temperature)^2 only. Consequently, the most vital factor influences the response variables is melt temperature followed by squeeze pressure and die temperature.

Table 8 Summary of main, interaction and quadratic factors affecting the ultimate tensile strength and hardness

Factors	Ultimate tensile strength (MPa)		Hardness (HV)	
	As-casted	Aged	As-casted	Aged
Squeeze pressure: A	✓	✓	✓	✓
Die temperature: B	✓	✓	✓	✓
Melt temperature: C	✓	✓	✓	✓
Squeeze pressure × die temperature: AB				
Squeeze pressure × melt temperature: AC			✓	✓
Die temperature × melt temperature: BC		✓	✓	✓
(Squeeze pressure)^2: A^2	✓	✓	✓	✓
(Die temperature)^2: B^2				✓
(Melt temperature)^2: C^2	✓	✓	✓	✓

3.4 Comparison of as-casted and aged 2024-2024 overcast joints responses

The discussion in the previous sections clearly highlights that aged overcast joints results in better ultimate tensile strength and hardness as compared to as-casted overcast joints. To further demonstrate the effectiveness of aged overcast joints,

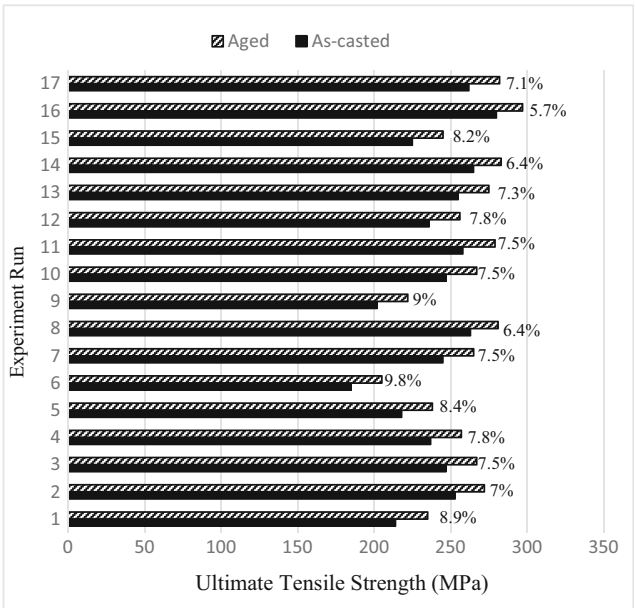

Fig. 10 Comparison of ultimate tensile strength (as-casted) and (aged) results

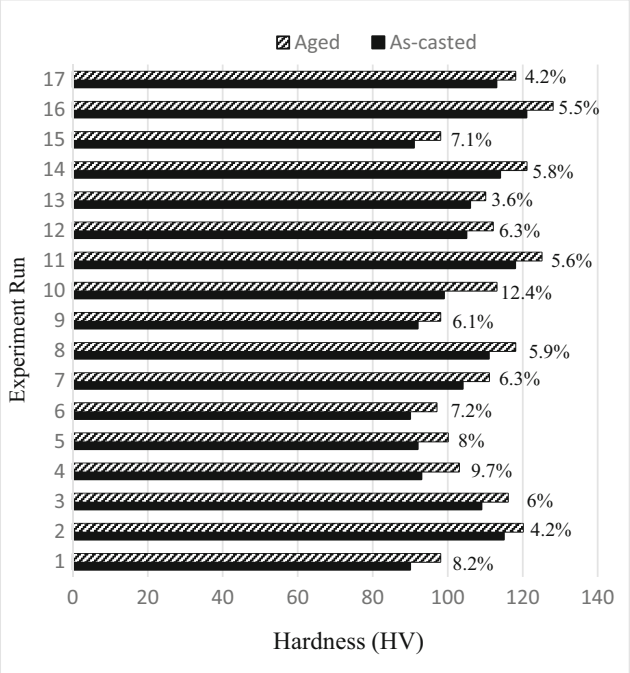

Fig. 11 Comparison of hardness (as-casted) and (aged) results

comparison between both conditions is provided in Figs. 10 and 11. It must be noted that the values of response variables have been drawn from the design space provided in Table 4. It is evident from the figures (Figs. 10 and 11) that improvement in ultimate tensile strength and hardness has been observed in the range of 5.7~9.8 and 3.6~12.4%, respectively, for age overcast joints.

The effectiveness of squeeze overcasting can be observed by comparing maximum ultimate tensile strength and hardness obtained through squeeze overcasting with the corresponding values of base metal itself (Fig. 12). It is clearly evident from Fig. 12 that 40 and 48.5% improvement in ultimate tensile strength has been achieved for as-casted and aged overcasted joints, respectively. Similarly, 39 and 47% improvement in hardness has been achieved through as-casted and overcasting, respectively. These significant differences in ultimate tensile strength and hardness clearly justify the deployment of squeeze pressure during overcasting.

4 Conclusions

The aim of this research was to evaluate and improve ultimate tensile strength and hardness of squeeze casted Al-Al joints under as-casted and aged overcasting conditions. This has been achieved through detailed investigation of the effects of squeeze pressure, die temperature and melt temperature on as-casted and aged overcasted joints. Response surface methodology has been used to design experiments and develop empirical models of ultimate tensile strength and hardness. The following conclusions can be drawn from this research:

- For both as-casted and aged overcast conditions, melt temperature has been identified as the most significant process parameters affecting the ultimate tensile strength and hardness.
- Maximum ultimate tensile strength and hardness can be achieved near the middle levels of melt temperature and squeeze pressure and at the highest level of die temperature.
- The comparison of the developed empirical models for both overcasting conditions revealed that aged overcasting has a tendency to increase ultimate tensile strength and hardness by 9.8 and 12.4%, respectively as compared to overcasting under as-casted condition.

The findings of this research will aid the manufacturing industries in developing lightweight materials with excellent mechanical properties.

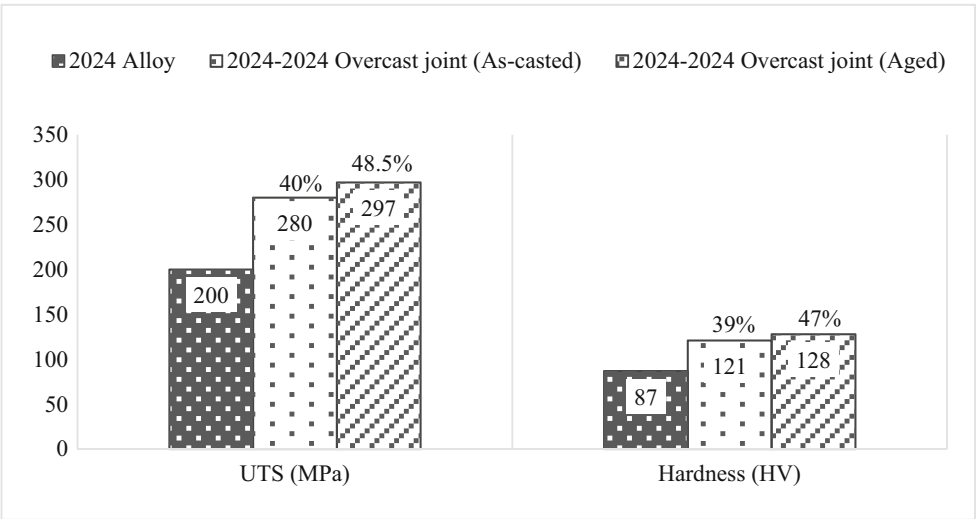

Fig. 12 Comparison of Al 2024-2024 overcast joint (as-casted and aged) with base metal (Al 2024 alloy)

References

1. Williams JC, Starke EA (2003) Progress in structural materials for aerospace systems. Acta Mater 51(19):5775–5799. https://doi.org/10.1016/j.actamat.2003.08.023
2. Taub AI, Krajewski PE, Luo AA, Owens JN (2007) The evolution of technology for materials processing over the last 50 years: the automotive example. JOM J Miner Met Mater Soc 59(2):48–57. https://doi.org/10.1007/s11837-007-0022-7
3. Liu T, Wang Q, Sui Y, Wang Q (2016) Microstructure and mechanical properties of overcast 6101–6101 wrought al alloy joint by squeeze casting. J Mater Sci Technol 32(4):298–304. https://doi.org/10.1016/j.jmst.2015.11.020
4. Chang S et al (2009) Joining 6061 aluminum alloy with al–Si–cu filler metals. J Alloys Compd 488(1):174–180. https://doi.org/10.1016/j.jallcom.2009.08.056
5. Lee K et al (2013) Influence of reduction ratio on the interface microstructure and mechanical properties of roll-bonded Al/Cu sheets. Mater Sci Eng A 583:177–181. https://doi.org/10.1016/j.msea.2013.06.077
6. Xue P, Ni DR, Wang D, Xiao BL, Ma ZY (2011) Effect of friction stir welding parameters on the microstructure and mechanical properties of the dissimilar Al–Cu joints. Mater Sci Eng A 528(13):4683–4689. https://doi.org/10.1016/j.msea.2011.02.067
7. Chang C et al (2010) Effect of laser welding on properties of dissimilar joint of Al-Mg-Si and Al-Mn aluminum alloys. J Mater Sci Technol 26(3):276–282. https://doi.org/10.1016/S1005-0302(10)60046-1
8. Honarpisheh M, Asemabadi M, Sedighi M (2012) Investigation of annealing treatment on the interfacial properties of explosive-welded Al/Cu/Al multilayer. Mater Des 37:122–127. https://doi.org/10.1016/j.matdes.2011.12.045
9. Akatsu T, Hosoda N, Suga T, Rühle M (1999) Atomic structure of Al/Al interface formed by surface activated bonding. J Mater Sci 34(17):4133–4139. https://doi.org/10.1023/A:1004661610307
10. Lee T et al (2013) Controlling Al/Cu composite diffusion layer during hydrostatic extrusion by using colloidal Ag. J Mater Process Technol 213(3):487–494. https://doi.org/10.1016/j.jmatprotec.2012.10.001
11. Yu Z, Duan Y, Liu L, Liu S, Liu X, Li X (2009) Growth behavior of Cu/Al intermetallic compounds in hot-dip aluminized copper. Surf Interface Anal 41(5):361–365. https://doi.org/10.1002/sia.3020
12. Liu T, Wang Q, Sui Y, Wang Q, Ding W (2016) An investigation into interface formation and mechanical properties of aluminum–copper bimetal by squeeze casting. Mater Des 89:1137–1146. https://doi.org/10.1016/j.matdes.2015.10.072
13. Sun J, Song X, Wang T, Yu Y, Sun M, Cao Z, Li T (2012) The microstructure and property of Al–Si alloy and Al–Mn alloy bimetal prepared by continuous casting. Mater Lett 67(1):21–23. https://doi.org/10.1016/j.matlet.2011.08.112
14. Wang T, Liang C, Chen Z, Zheng Y, Kang H, Wang W (2014) Development of an 8090/3003 bimetal slab using a modified direct-chill casting process. J Mater Process Technol 214(9):1806–1811. https://doi.org/10.1016/j.jmatprotec.2014.03.029
15. Hajjari E, Divandari M, Razavi SH, Emami SM, Homma T, Kamado S (2011) Dissimilar joining of Al/Mg light metals by compound casting process. J Mater Sci 46(20):6491–6499. https://doi.org/10.1007/s10853-011-5595-4
16. Papis K et al (2008) Interface formation in aluminium–aluminium compound casting. Acta Mater 56(13):3036–3043. https://doi.org/10.1016/j.actamat.2008.02.042
17. Viala J et al (2002) Interface chemistry in aluminium alloy castings reinforced with iron base inserts. Compos A: Appl Sci Manuf 33(10):1417–1420. https://doi.org/10.1016/S1359-835X(02)00158-6
18. Liu H et al (2006) Interfacial strength and structure of stainless steel–semi-solid aluminum alloy clad metal. Mater Lett 60(2):180–184. https://doi.org/10.1016/j.matlet.2005.08.015
19. Şimşir M, Kumruoğlu LC, Özer A (2009) An investigation into stainless-steel/structural-alloy-steel bimetal produced by shell mould casting. Mater Des 30(2):264–270. https://doi.org/10.1016/j.matdes.2008.04.074
20. Xu G, Luo AA, Chen Y, Sachdev AK (2014) Interfacial phenomena in magnesium/aluminum bi-metallic castings. Mater Sci Eng A 595:154–158. https://doi.org/10.1016/j.msea.2013.11.093
21. Paramsothy M, Srikanth N, Gupta M (2008) Solidification processed Mg/Al bimetal macrocomposite: microstructure and mechanical properties. J Alloys Compd 461(1):200–208. https://doi.org/10.1016/j.jallcom.2007.07.050
22. Xiong B, Cai C, Wan H, Lu B (2011) Fabrication of high chromium cast iron and medium carbon steel bimetal by liquid–solid casting in electromagnetic induction field. Mater Des 32(5):2978–2982. https://doi.org/10.1016/j.matdes.2011.01.006
23. Xiong B, Cai C, Lu B (2011) Effect of volume ratio of liquid to solid on the interfacial microstructure and mechanical properties of high chromium cast iron and medium carbon steel bimetal. J Alloys Compd 509(23):6700–6704. https://doi.org/10.1016/j.jallcom.2011.03.142
24. Hejazi MM, Divandari M, Taghaddos E (2009) Effect of copper insert on the microstructure of gray iron produced via lost foam casting. Mater Des 30(4):1085–1092. https://doi.org/10.1016/j.matdes.2008.06.032
25. Papis K, Löffler J, Uggowitzer P (2010) Interface formation between liquid and solid Mg alloys—An approach to continuously metallurgic joining of magnesium parts. Mater Sci Eng A 527(9):2274–2279. https://doi.org/10.1016/j.msea.2009.11.066
26. Zhang H, Chen Y, Luo AA (2014) A novel aluminum surface treatment for improved bonding in magnesium/aluminum bimetallic castings. Scr Mater 86:52–55. https://doi.org/10.1016/j.scriptamat.2014.05.007
27. Hajjari E, Divandari M (2008) An investigation on the microstructure and tensile properties of direct squeeze cast and gravity die cast 2024 wrought Al alloy. Mater Des 29(9):1685–1689. https://doi.org/10.1016/j.matdes.2008.04.012
28. Koerner C, Schwankl M, Himmler D (2014) Aluminum–aluminum compound castings by electroless deposited zinc layers. J Mater Process Technol 214(5):1094–1101. https://doi.org/10.1016/j.jmatprotec.2013.12.014
29. Rübner M, Günzl M, Körner C, Singer RF (2011) Aluminium–aluminium compound fabrication by high pressure die casting. Mater Sci Eng A 528(22):7024–7029. https://doi.org/10.1016/j.msea.2011.05.076
30. Ghomashchi M, Vikhrov A (2000) Squeeze casting: an overview. J Mater Process Technol 101(1):1–9
31. Liu T, Wang Q, Sui Y, Wang Q, Ding W (2015) An investigation into aluminum–aluminum bimetal fabrication by squeeze casting. Mater Des 68:8–17. https://doi.org/10.1016/j.matdes.2014.11.051
32. Zhang Y, Ji S, Scamans G, Fan Z (2017) Interfacial characterisation of overcasting a cast Al-Si-Mg (A356) alloy on a wrought Al-Mg-Si (AA6060) alloy. J Mater Process Technol 243:197–204. https://doi.org/10.1016/j.jmatprotec.2016.12.022
33. Haider KMA, Mufti NA (2014) Mechanical and microstructural evaluation of squeeze cast Al-4% Cu alloy using a full-factorial experimental design. JOM 66(8):1446–1453. https://doi.org/10.1007/s11837-014-0973-4
34. Souissi N, Souissi S, Lecompte JP, Amar MB, Bradai C, Halouani F (2015) Improvement of ductility for squeeze cast 2017 A wrought aluminum alloy using the Taguchi method. Int J Adv Manuf Technol 78(9–12):2069–2077. https://doi.org/10.1007/s00170-015-6792-0

35. Vijian P, Arunachalam V (2007) Optimization of squeeze casting process parameters using Taguchi analysis. Int J Adv Manuf Technol 33(11):1122–1127. https://doi.org/10.1007/s00170-006-0550-2
36. Senthil P, Amirthagadeswaran K (2012) Optimization of squeeze casting parameters for non symmetrical AC2A aluminium alloy castings through Taguchi method. J Mech Sci Technol 26(4): 1141–1147. https://doi.org/10.1007/s12206-012-0215-z
37. Vijian P, Arunachalam V (2007) Modelling and multi objective optimization of LM24 aluminium alloy squeeze cast process parameters using genetic algorithm. J Mater Process Technol 186(1):82–86. https://doi.org/10.1016/j.jmatprotec.2006.12.019
38. Senthil P, Amirthagadeswaran K (2014) Experimental study and Squeeze Casting Process Optimization for High Quality AC2A Aluminium Alloy Castings. Arab J Sci Eng (Springer Science & Business Media BV) 39(3)
39. Patel GM, Krishna P, Parappagoudar MB (2014) Optimization of squeeze cast process parameters using Taguchi and grey relational analysis. Procedia Technol 14:157–164. https://doi.org/10.1016/j.protcy.2014.08.021
40. Manjunath Patel G, Krishna P, Parappagoudar MB (2016) Modelling and multi-objective optimisation of squeeze casting process using regression analysis and genetic algorithm. Aust J Mech Eng 14(3):182–198. https://doi.org/10.1080/14484846.2015.1093231
41. Patel GCM, Krishna P, Parappagoudar M (2015) Modelling of squeeze casting process using design of experiments and response surface methodology. Int J Cast Met Res 28(3):167–180. https://doi.org/10.1179/1743133614Y.0000000144
42. Sarfraz S, Jahanzaib M, Wasim A, Hussain S, Aziz H (2017) Investigating the effects of as-casted and in situ heat-treated squeeze casting of Al-3.5% Cu alloy. Int J Adv Manuf Technol 89(9–12):3547–3561. https://doi.org/10.1007/s00170-016-9350-5
43. Patel GM et al (2014) Investigation of squeeze cast process parameters effects on secondary dendrite arm spacing using statistical regression and artificial neural network models. Procedia Technol 14:149–156. https://doi.org/10.1016/j.protcy.2014.08.020
44. Patel M, Krishna P, Parappagoudar MB (2015) Prediction of secondary dendrite arm spacing in squeeze casting using fuzzy logic based approaches. Arch Foundry Eng 15(1):51–68
45. Karnik S, Gaitonde V, Davim J (2008) A comparative study of the ANN and RSM modeling approaches for predicting burr size in drilling. Int J Adv Manuf Technol 38(9):868–883. https://doi.org/10.1007/s00170-007-1140-7
46. Montgomery DC (2017) Design and analysis of experiments. John Wiley & Sons
47. Manjunath Patel GC, Krishna P, Parappagoudar MB (2016) Squeeze casting process modeling by a conventional statistical regression analysis approach. Appl Math Model 40(15):6869–6888
48. Dursun T, Soutis C (2014) Recent developments in advanced aircraft aluminium alloys. Mater Des 56:862–871. https://doi.org/10.1016/j.matdes.2013.12.002
49. Qi G, Chen X, Shao Z (2002) Influence of bath chemistry on zincate morphology on aluminum bond pad. Thin Solid Films 406(1):204–209. https://doi.org/10.1016/S0040-6090(01)01714-X
50. Saito M, Maegawa T, Homma T (2005) Electrochemical analysis of zincate treatments for Al and Al alloy films. Electrochim Acta 51(5):1017–1020. https://doi.org/10.1016/j.electacta.2005.05.063
51. Teng L et al (2015) Microstructure and mechanical properties of overcast aluminum joints. Trans Nonferrous Metals Soc China 25(4):1064–1072
52. Kasman Ş, Saklakoglu IE (2012) Determination of process parameters in the laser micromilling application using Taguchi method: a case study for AISI H13 tool steel. Int J Adv Manuf Technol 58(1): 201–209. https://doi.org/10.1007/s00170-011-3371-x
53. Mia M, Razi MH, Ahmad I, Mostafa R, Rahman SMS, Ahmed DH, Dey PR, Dhar NR (2017) Effect of time-controlled MQL pulsing on surface roughness in hard turning by statistical analysis and artificial neural network. Int J Adv Manuf Technol 91(1–13):3211–3223. https://doi.org/10.1007/s00170-016-9978-1
54. Hassan M, Othman A, Kamaruddin S (2017) The use of response surface methodology (RSM) to optimize the acid digestion parameters in fiber volume fraction test of aircraft composite structures. Int J Adv Manuf Technol 90(9–12):3739–3748. https://doi.org/10.1007/s00170-016-9683-0
55. Deng J (1988) Essential topics on grey system: theory and applications. China Ocean Press
56. Mia M, Bashir MA, Khan MA, Dhar NR (2017) Optimization of MQL flow rate for minimum cutting force and surface roughness in end milling of hardened steel (HRC 40). Int J Adv Manuf Technol 89(1–4):675–690. https://doi.org/10.1007/s00170-016-9080-8
57. Mia M, Dhar NR (2016) Response surface and neural network based predictive models of cutting temperature in hard turning. J Adv Res 7(6):1035–1044. https://doi.org/10.1016/j.jare.2016.05.004
58. Bouacha K, Yallese MA, Mabrouki T, Rigal JF (2010) Statistical analysis of surface roughness and cutting forces using response surface methodology in hard turning of AISI 52100 bearing steel with CBN tool. Int J Refract Met Hard Mater 28(3):349–361. https://doi.org/10.1016/j.ijrmhm.2009.11.011
59. Jahanzaib M, Hussain S, Wasim A, Aziz H, Mirza A, Ullah S (2017) Modeling of weld bead geometry on HSLA steel using response surface methodology. Int J Adv Manuf Technol 89(5–8): 2087–2098. https://doi.org/10.1007/s00170-016-9213-0
60. Azam M, Jahanzaib M, Wasim A, Hussain S (2015) Surface roughness modeling using RSM for HSLA steel by coated carbide tools. Int J Adv Manuf Technol 78(5-8):1031–1041. https://doi.org/10.1007/s00170-014-6707-5
61. Nami H, Halvaee A, Adgi H, Hadian A (2010) Investigation on microstructure and mechanical properties of diffusion bonded Al/Mg 2 Si metal matrix composite using copper interlayer. J Mater Process Technol 210(10):1282–1289. https://doi.org/10.1016/j.jmatprotec.2010.03.015